Identification of the Cysteine Residue Exposed by the Conformational Change in Pig Heart Succinyl-CoA:3-Ketoacid Coenzyme A Transferase on Binding Coenzyme A[†,‡]

Stephanie D. Tammam,[§,||,⊥] Jean-Christophe Rochet,[§,#] and Marie E. Fraser*[,||]

Department of Biological Sciences, University of Calgary, 2500 University Drive NW, Calgary, Alberta T2N 1N4, Canada, and Department of Biochemistry, University of Alberta, Edmonton, Alberta T6G 2H7, Canada

Received May 1, 2007; Revised Manuscript Received July 18, 2007

ABSTRACT: Succinyl-CoA:3-ketoacid CoA transferase (SCOT) transfers CoA from succinyl-CoA to acetoacetate via a thioester intermediate with its active site glutamate residue, Glu 305. When CoA is linked to the enzyme, a cysteine residue can now be rapidly modified by 5,5′-dithiobis(2-nitrobenzoic acid), reflecting a conformational change of SCOT upon formation of the thioester. Since either Cys 28 or Cys 196 could be the target, each was mutated to Ser to distinguish between them. Like wild-type SCOT, the C196S mutant protein was modified rapidly in the presence of acyl-CoA substrates. In contrast, the C28S mutant protein was modified much more slowly under identical conditions, indicating that Cys 28 is the residue exposed on binding CoA. The specific activity of the C28S mutant protein was unexpectedly lower than that of wild-type SCOT. X-ray crystallography revealed that Ser adopts a different conformation than the native Cys. A chloride ion is bound to one of four active sites in the crystal structure of the C28S mutant protein, mimicking substrate, interacting with Lys 329, Asn 51, and Asn 52. On the basis of these results and the studies of the structurally similar CoA transferase from *Escherichia coli*, YdiF, bound to CoA, the conformational change in SCOT was deduced to be a domain rotation of 17° coupled with movement of two loops: residues 321−329 that bury Cys 28 and interact with succinate or acetoacetate and residues 374−386 that interact with CoA. Modeling this conformational change has led to the proposal of a new mechanism for catalysis by SCOT.

Succinyl-CoA:3-ketoacid coenzyme A transferase (SCOT)[1] is an essential enzyme in the metabolism of ketone bodies (acetoacetate and β-hydroxybutyrate) in higher animals. Ketone bodies are produced from the catabolism of fatty acids in the liver and serve as a source of energy for many tissues, including the heart, since they can be transported through the blood stream. In the mitochondria of these recipient tissues, SCOT activates acetoacetate by transferring the CoA group from succinyl-CoA to acetoacetate to produce acetoacetyl-CoA and succinate (*1*): succinyl-CoA + acetoacetate ⇔ succinate + acetoacetyl-CoA. Acetoacetyl-CoA is further catabolized to acetyl-CoA, which enters the citric acid cycle to provide energy.

The initial experiments characterizing SCOT were performed on protein purified from pig heart (*2*). The pig heart enzyme has long been known to exist as a homodimer (*3*), but there is also a homotetrameric form with identical specific activity (*4*). A glutamate residue, identified as Glu 305 (*5*), lies at each active site of the enzyme and forms a thioester bond with CoA as part of the catalytic mechanism (*6*). The formation of the thioester takes place through an anhydride intermediate, as demonstrated by monitoring the exchange of an oxygen atom between the active site glutamate residue and succinate (*7*). The reaction proceeds via ping-pong kinetics with succinate leaving before acetoacetate can be bound (*8*). The reaction pathway can be summarized as succinyl-CoA + Glu ⇔ CoA + Glu-succinate (anhydride)

[†] Our research was supported by the Canadian Institutes of Health Research, Grant MOP-42446, and made use of equipment funded by the Natural Sciences and Engineering Research Council of Canada and the Alberta Heritage Foundation for Medical Research (AHFMR). X-ray diffraction data were collected at beamlines 8.3.1 and 12.3.1 of the Advanced Light Source (ALS) at Lawrence Berkeley Laboratory, under an agreement with the Alberta Synchrotron Institute (ASI). The ALS is operated by the Department of Energy and supported by the National Institutes of Health. Beamline 8.3.1 was funded by the National Science Foundation, the University of California, and Henry Wheeler. SIBYLS (beamline 12.3.1) was funded by NCI Grant CA92584 and DOE Contract DE-AC03-76SF00098. The ASI synchrotron access program is supported by grants from the Alberta Science and Research Authority and AHFMR. M.E.F. is a Biomedical Scholar supported by AHFMR. S.D.T.'s contributions to this work formed part of her M.Sc. research. J.-C.R.'s contributions to this work formed part of his Ph.D. research.

[‡] Protein Data Bank identifiers are 2NRB and 2NRC.

* To whom correspondence should be addressed. E-mail: frasm@ucalgary.ca. Phone: 403-220-6145. Fax: 403-289-9311.

[§] These authors contributed equally to this work.

[||] University of Calgary.

[⊥] Current address: Department of Molecular Structure and Function, Hospital for Sick Children, Black Wing Room 3333, 555 University Ave., Toronto, Ontario M5G 1X8, Canada.

[#] University of Alberta. Current address: Department of Medicinal Chemistry and Molecular Pharmacology, Purdue University, West Lafayette, IN 47907.

[1] Abbreviations: AA, acetoacetate; AACoA, acetoacetyl-CoA; DTNB, 5,5′-dithiobis(2-nitrobenzoic acid); DTT, dithiothreitol; E−CoA, enzyme−thioester intermediate; NTCB, 2-nitro-5-(thiocyanato)benzoic acid; RCoA, acyl-CoA; rmsd, root mean squared deviation; SCOT, succinyl-CoA:3-ketoacid coenzyme A transferase; Succ, succinate; SCoA, succinyl-CoA; TNB, thionitrobenzoic acid.

10.1021/bi700828h CCC: $37.00
Published on Web 08/24/2007

⇔ succinate + Glu-CoA (thioester); acetoacetate + Glu-CoA (thioester) ⇔ CoA + Glu-acetoacetate (anhydride) ⇔ acetoacetyl-CoA + Glu where Glu is the active site residue of SCOT.

Experiments involving the chemical modification of cysteine residues in SCOT provided evidence of a conformational change occurring upon binding the CoA group. The free enzyme is slowly inactivated by the thiol-modifying reagent, 5,5′-dithiobis(2-nitrobenzoic acid) (DTNB), but inactivation of the enzyme−thioester intermediate, E−CoA, involves two phases, one rapid and reversible, the other slow and irreversible (*9*). The rapid loss of enzyme activity was shown to be due to modifying a single cysteine residue of each monomer. To prove that the reactive cysteine was not a catalytic residue, Kindman and Jencks repeated the chemical modification experiments using a different thiol-modifying reagent, 2-nitro-5-(thiocyanato)benzoic acid (NTCB), that could label the cysteine with either the large 2-nitro-5-thiobenzoic acid group or the smaller cyano group (*10*). Adding the small group did not inactivate the enzyme, leading to the interpretation that the covalent modification of one particular cysteine residue, Cys X, by bulky thiol reagents resulted in steric hindrance at the active site, the cause of lower activity (*9*, *10*). Chemical modification and peptide sequencing experiments distinguished five cysteine residues (*11*) that were identified as Cys 28, Cys 196, Cys 417, Cys 426, and Cys 465 once the gene was cloned (*12*). To discriminate among the five, Williams followed up on the chemical modification experiments by using peptide sequencing to identify two cysteine residues, now known to be Cys 28 and Cys 196, as the main ones modified upon prolonged incubation with [^{14}C]-*N*-ethylmaleimide in the presence of acetoacetyl-CoA (*11*). One of these two cysteine residues was modified via the rapid pathway, whereas the other reacted more slowly, indicating that either Cys 28 or Cys 196 must be Cys X. Identification of Cys X would provide an understanding of the conformational change, an important step in deciphering the catalytic mechanism of SCOT.

The crystal structure of SCOT shows the locations of Glu 305, the active site glutamate residue, Cys 28, and Cys 196 in each subunit of the homodimer (*13*), so it could help in the identification of Cys X. Glu 305 is located near the center of the monomer at the base of an open funnel (*13*). Neither Cys 28 nor Cys 196 is located in the funnel so it is not obvious how the covalent modification of either residue would lead to steric hindrance at the active site. However, SCOT was crystallized in the free form, and the rapid, reversible inactivation by chemical modification of Cys X requires that the enzyme be covalently bound to CoA.

Structures of a CoA transferase from *Escherichia coli*, YdiF, have been determined crystallographically both in the free form and covalently bound to CoA (*14*). Since YdiF has a similar fold to SCOT, comparisons of the structures of YdiF could show what conformational change must occur in SCOT on binding CoA. However, in the case of YdiF, no major differences were observed in the conformation of the enzyme on binding CoA (*14*). This would suggest either that there is no conformational change occurring when YdiF binds CoA or that CoA-free YdiF has been trapped in the CoA-binding conformation during crystallization. Furthermore, YdiF does not have a Cys residue in a similar position to Cys 28 or Cys 196 of SCOT, so the chemical modification experiments cannot be repeated with YdiF without using site-directed mutagenesis to insert a cysteine residue.

Site-directed mutagenesis of SCOT can be used to distinguish between Cys 28 and Cys 196 and identify Cys X, and that research is described here. It was predicted that the replacement of sulfur by oxygen in the side chain of residue 28 or 196 should not alter the catalytic function of SCOT, so each of these cysteine residues was changed to serine and the experiments with DTNB were performed with the mutant proteins to see which would be rapidly modified in the presence of acetoacetyl-CoA. If the C28S mutant protein were still rapidly modified, then residue 196 must be Cys X, while if the C196S mutant protein were rapidly modified, then residue 28 must be Cys X. The C28S and C196S mutant proteins were tested for catalytic activity, and both were active, but the C28S mutant was less active than wild-type SCOT. To investigate why there was this loss of activity, Cys 28 was also mutated to Ala, essentially removing the sulfur atom. Kinetic analyses were performed with both of the Cys 28 mutant proteins, and the structure of each was determined using X-ray crystallography. On the basis of the identification of Cys 28 as the cysteine residue exposed on linking CoA to SCOT and the structure of YdiF covalently linked to CoA, the structure of SCOT has been modeled in the alternate conformation. The conformational change has been included in a new description of the catalytic mechanism of SCOT.

EXPERIMENTAL PROCEDURES

Site-Directed Mutagenesis, Gene Expression, and Protein Purification. Three mutations were made in the pT7-7 plasmid encoding SCOT (*15*). To change Cys 28 or Cys 196 to serine, mutations were made using an M13 vector (*16*), and to change Cys 28 to alanine, the mutation was made using the QuikChange XL kit from Stratagene. The oligonucleotides used for the mutagenesis were 5′-GTTTTGGGTTATCTGGAATTCCGG-3′ for C28S, 5′-ACCTGCCGATGTCCAAAGCTGCAG-3′ for C196S, and 5′-GGTTGGTGGTTTTGGGTTAGCCGGAATTCCGGAGAATCTTATAGG-3′ and its complement for C28A. When using the M13 vector, the mutated plasmid was created in two steps to ensure that much of the cDNA insert was free of mutations due to misincorporation by *Thermus aquaticus* polymerase. After making the mutation in the M13 vector, the gene was cleaved and subcloned into the expression vector using the restriction enzyme sites for *Xba*I and *Hin*dIII to transfer the 1.5 kb segment that included the full length of the gene. In the second step for the C28S mutant, a *Bam*HI restriction enzyme site 3′ to the site of the mutation was used to cleave the 1.2 kb *Bam*HI−*Hin*dIII segment and replace it with the equivalent region excised from the plasmid encoding wild-type SCOT. For the C196S mutant, the 0.6 kb *Msc*I−*Hin*dIII segment was cleaved and replaced with the equivalent region excised from the plasmid encoding wild-type SCOT. The QuikChange XL kit was used essentially as described in the instructions, except that the modification of Wang and Malcolm was followed to reduce dimerization of the mutagenic primers (*17*). In the modified procedure, half of the plasmid sample was mixed with each primer and one-third of the polymerase and subjected to 10 cycles of chain elongation, before the samples were mixed and the final third

of the polymerase was added. The standard protocol for chain elongation was then followed. In all cases, the sequence of the mutated gene was confirmed by automated sequence determinations (*18*).

For protein expression, electrocompetent or Inoue competent (*19*) BL21(DE3) cells were transformed with the pT7-7 vectors. *E. coli* producing the C28S mutant protein were grown in 10 L of Luria−Bertani broth incubated in a fermenter unit with vigorous aeration. The other mutant proteins were produced in two to four 2.8 L Fernbach flasks with 1 L of Luria−Bertani broth per flask. In each case, an overnight culture was used to inoculate the broth and allowed to grow at 37 °C to an optical density of 0.6 measured at 600 nm prior to induction. Protein production was induced with 0.1 mM isopropyl β-D-thiogalactopyranoside, and the culture was left to grow overnight at 21 °C. The cells were harvested by centrifugation and frozen at −80 °C prior to protein purification. The mutant proteins were purified essentially as described for the wild-type protein (*15*) or for the selenomethionine version of the protein (*13*), leading to similarly pure protein. Optimally, a 10 L culture yielded 50 mg of the C28S mutant protein in pure form, while the cultures in Fernbach flasks yielded 10 mg. The homogeneity of each protein preparation was confirmed by SDS−PAGE analysis.

Enzyme Activity and Kinetic Assays. The specific SCOT activity was determined spectrophotometrically at 21−22 °C by measuring the production of acetoacetyl-CoA in an assay solution containing 15 mM $MgCl_2$, 0.30 mM succinyl-CoA, 67 mM acetoacetate, and 50 mM Tris-HCl, pH 9.1. The concentration of succinyl-CoA was measured by absorption using the extinction coefficient at 232 nm of 4.50×10^3 M^{-1} cm^{-1} for a solution of the substrate freshly prepared in 0.10 M Tris-HCl, 10 mM $MgCl_2$, 0.1 M KCl, and 10 mM sodium succinate at pH 7.5 (*20*). The extinction coefficient for acetoacetyl-CoA at 310 nm under these conditions was taken to be 7.8×10^3 M^{-1} cm^{-1} (*21*). The protein concentration was measured by absorption at 278 nm uncorrected for light scattering using the extinction coefficient of 0.75 $(mg/mL)^{-1}$. This extinction coefficient was experimentally determined on the basis of the extinction coefficient of 0.65 $(mg/mL)^{-1}$ when the absorbance measurements were corrected for scatter (*15*).

Kinetics measurements were performed at 21−22 °C using previously published procedures (*8*, *22*). The formation of succinyl-CoA from various concentrations of acetoacetyl-CoA (0.045−0.135 mM) and succinate (4.0−40 mM) was monitored by the decrease in absorbance at 310 nm in an assay solution of 0.067 M Tris−SO_4 buffer, pH 8.1. The ionic strength of the reaction mixture was adjusted to 1.0 M by the addition of the appropriate amount of Na_2SO_4 since high ionic strength increases the ionization of acetoacetyl-CoA to the enolate form (*8*). An extinction coefficient at 310 nm of 5.20×10^3 M^{-1} cm^{-1}, identical to that reported (*23*), was measured for acetoacetyl-CoA under these conditions. The accuracy of this assay requires consideration of two external factors. First, reaction mixtures lacking enzyme consistently showed a spontaneous decrease in absorbance with time of incubation. This spontaneous decrease occurred at a progressively slower rate, reaching a minimum after approximately 5 min, so the enzyme was added after the decrease occurred at a constant rate, which was then subtracted from the rate of the catalyzed reaction. From separate measurements, it was demonstrated that less than 3% of the initial acetoacetyl-CoA hydrolyzed spontaneously during this period. Second, the observed SCOT activity decreased with first-order kinetics during the time of the assay. To correct for this decrease, the initial rate was estimated from a plot of "log enzyme activity versus time" by extrapolating to zero time. The enzyme activity was shown to be proportional to the concentration of the C28S mutant protein up to a concentration of 0.32 μg/mL.

The formation of acetoacetyl-CoA from higher concentrations of succinyl-CoA (0.284−1.14 mM) and acetoacetate (0.018−0.18 mM) could not be measured directly due to product inhibition (*8*). Instead, these reactions were coupled to the reduction of acetoacetyl-CoA by L-3-hydroxyacyl-CoA dehydrogenase. This reduction was monitored by the decrease in absorbance at 340 nm, reflecting the disappearance of NADH. The assay solution consisted of 0.061 M Tris−SO_4 buffer, 0.14 mM NADH, 0.29 M Na_2SO_4, and 10 μg of L-3-hydroxyacyl-CoA dehydrogenase at pH 8.1. L-3-Hydroxyacyl-CoA dehydrogenase, either the pig heart enzyme supplied as an ammonium sulfate suspension (Sigma-Aldrich Co.) or the human enzyme expressed and purified from *E. coli* (*24*), was dialyzed against 0.5 L of 10 mM Tris-HCl, 1 mM EDTA, and 2 mM 2-mercaptoethanol (pH 8.0) prior to use. An extinction coefficient of 6.22×10^3 M^{-1} cm^{-1} was used for NADH under these conditions (*8*, *25*). The rate of the catalyzed reaction was corrected for the spontaneous decrease in absorbance of reaction mixtures lacking SCOT. The SCOT activity was shown to be linear with respect to the concentration of enzyme up to 4.0 μg/mL of C28S.

The raw spectrophotometric data from kinetic assays were fit to single-exponential curves using the program TableCurve 2D (Jandel Scientific, San Rafael, CA). Kinetic parameters were derived from these data using standard replotting methods for a ping-pong bi-bi reaction as described by Segel (*26*). All standard errors were calculated using accepted formulas for the propagation of error (*27*).

Modification by DTNB (Loss of SCOT Activity). Samples of purified wild-type SCOT, C28S, or C196S were treated with DTNB as described previously for wild-type SCOT by White et al. (*9*). Prior to the analysis, the proteins were dialyzed against 20 mM Tris-HCl, pH 8.0, and diluted in 0.8 mM EDTA and 0.2 M Tris-HCl, pH 8.0. The final protein concentration was 0.21 mg/mL (wild-type), 0.64 mg/mL (C28S), or 0.24 mg/mL (C196S). In some cases the reaction mixture also contained succinyl-CoA, succinyl-CoA plus succinate, acetoacetyl-CoA, or acetoacetyl-CoA plus acetoacetate. The acyl-CoA and acyl substrates were included at a 2-fold or 1000-fold molar excess, respectively, relative to the number of active sites. DTNB was added last to the reaction mixture at a final concentration of 0.4 mM, and aliquots were removed at various times and assayed for SCOT activity. For these experiments, the enzyme assay solution consisted of 5 mM $MgSO_4$, 0.30 mM succinyl-CoA, 67 mM acetoacetate, and 67 mM Tris−SO_4, pH 8.1 [these conditions were adapted from White et al. (*9*)].

The reversibility of the inactivation by DTNB was assessed by adding dithiothreitol (DTT) at a final concentration of 2 mM to aliquots removed from the reaction mixture at different times. These aliquots were then incubated under an atmosphere enriched in nitrogen for 2 h at 22 °C prior to

being assayed for SCOT activity. The nitrogen was included to decrease the frequency of inactivating oxidation reactions.

Modification by DTNB (Release of Thionitrobenzoic Acid). Samples of wild-type SCOT, C28S, or C196S were prepared and treated with DTNB in the absence or presence of succinyl-CoA, succinyl-CoA plus succinate, acetoacetyl-CoA, or acetoacetyl-CoA plus acetoacetate as described above. The final protein concentration was 0.16 mg/mL. DTNB was added last to the reaction mixture at a final concentration of 0.4 mM. The reaction of DTNB with cysteine thiols was assayed at 22 °C by monitoring the increase in A_{412} resulting from the release of thionitrobenzoic acid (TNB). The stoichiometry of the reaction between DTNB and wild-type or mutant SCOT was calculated assuming a molar extinction coefficient of 13600 M^{-1} cm^{-1} for TNB (*28*). Each experiment was carried out a minimum of two times.

Crystallography. Crystals were grown of the purified C28S and C28A mutant proteins so that their structures could be determined using X-ray diffraction. The mutant proteins were purified as described for the selenomethionine protein (*13*), so the samples contained between 0.125 and 0.5 M KCl in 0.5 mM benzamidine, 0.2 mM EDTA, 20 mM 2-mercaptoethanol, and 5 mM Tris-HCl, pH 8.0. They were crystallized at 14 °C in hanging drops using vapor diffusion. The precipitant solutions contained 14−22% polyethylene glycol 2000, 0.1 M Tris-HCl, pH 8.0, and 10−15% glycerol. The protein, at a concentration of at least 10 mg/mL, was added to a drop of the precipitant solution in a 1:1 ratio for a total drop volume of either 1 or 2 μL. Crystals often appeared within a day. The crystals were vitrified in a stream of nitrogen at 100 K and then stored in liquid nitrogen prior to shipment to the synchrotron for data collection.

Diffraction data were collected at the Advanced Light Source, Berkeley, CA. Data for the C28S mutant protein were collected at beamline 8.3.1, while data for the C28A mutant protein were collected at beamline 12.3.1. The diffraction images were analyzed using the HKL software (*29*). The starting model for the C28S mutant protein was the structure of SCOT with selenomethionine replacing the methionine residues (*13*). The model of the C28S mutant protein was subsequently used as the starting model for the C28A mutant protein. Programs from the CCP4 package were used for most of the crystallographic calculations (*30*). The program XFIT was used to visualize the electron density and the models and to rebuild the models (*31*). Five percent of the reflections were set aside to calculate R_{free} (*32*), the same reflections used for all data sets collected from this crystal form. The model was refined using the Crystallography and NMR Suite (CNS) (*33*) and checked after rounds of refinement using the programs WHATCHECK (*34*) and PROCHECK (*35*). The models were visualized and superposed using the programs O (*36*) and Swiss-PdbViewer (*37*). The models and the structure factor amplitudes were submitted to the Protein Data Bank (*38*) where they have been assigned the identifiers 2NRB and 2NRC for the C28S and C28A mutant proteins, respectively.

RESULTS

It had been predicted that the replacement of sulfur by oxygen in the side chain of residue 28 or 196 should not alter the catalytic function of SCOT since Cys X was not a catalytic residue. As expected, the specific activity of the C196S mutant protein, 22.4 ± 1.0 μmol min^{-1} mg^{-1}, was similar to that of wild-type SCOT, 25.2 ± 1.2 μmol min^{-1} mg^{-1}. Kinetic analyses were not done for the C196S mutant protein because of this result. However, the specific activity of the C28S mutant protein, 7.1 ± 0.2 μmol min^{-1} mg^{-1}, was 3.6 times lower than that of the wild-type enzyme. The kinetic constants determined for the C28S mutant protein (Table 1) showed that the reduction in specific activity compared to wild-type SCOT was due to a lower k_{cat} for the reaction between succinyl-CoA and acetoacetate, which was partially offset by lower K_M values for these substrates when compared to the wild-type enzyme. A kinetic analysis of the reaction between acetoacetyl-CoA and succinate catalyzed by the C28S mutant protein indicated that the K_M for succinate and k_{cat} were increased and decreased, respectively, compared to the wild-type enzyme.

Table 1: Kinetic Constants of Wild-Type and C28S and C28A Mutant Forms of SCOT

kinetic parameter	SCOT[a]	C28S mutant	C28A mutant
k_{cat}(forward)[b] ($\times 10^4$ min^{-1})	7.5 ± 0.4	4.9 ± 0.4	0.35 ± 0.5
K_M(acetoacetyl-CoA) (mM)	0.20 ± 0.04	0.10 ± 0.01	0.06 ± 0.01
K_M(succinate) (mM)	20 ± 4	39 ± 4	13 ± 3
k_{cat}(reverse)[c] ($\times 10^3$ min^{-1})	5.9 ± 0.4	0.55 ± 0.08	2.1 ± 0.4
K_M(succinyl-CoA) (mM)	6.5 ± 0.5	1.7 ± 0.3	8 ± 1
K_M(acetoacetate) (mM)	0.10 ± 0.03	0.05 ± 0.01	0.1 ± 0.3

[a] Reference *44*. [b] Forward reaction: acetoacetyl-CoA + succinate → succinyl-CoA + acetoacetate. [c] Reverse reaction: succinyl-CoA + acetoacetate → acetoacetyl-CoA + succinate.

To determine which cysteine residue could be rapidly modified by DTNB, samples of purified wild-type SCOT, C28S, and C196S were treated with DTNB in the absence or presence of succinyl-CoA, succinyl-CoA plus succinate, acetoacetyl-CoA, or acetoacetyl-CoA plus acetoacetate. The acyl-CoA substrates were included at a 2-fold molar excess relative to the number of active sites to ensure stoichiometric conversion of the enzyme to the thioester intermediate (*9*). The acyl substrates were included at a 1000-fold molar excess (combined with a 2-fold molar excess of acyl-CoA substrate) to promote the formation of a stable Michaelis complex (*9*). Wild-type SCOT and C196S were both inactivated by DTNB with more rapid kinetics in the presence of succinyl- or acetoacetyl-CoA (∼70−80% inactivation in 25 min) than in the absence of acyl-CoA (only ∼30% inactivation in 25 min and ∼40−50% inactivation in 50 min) (Figures 1 and 2). The increase in the inactivation rate induced by acyl-CoA was suppressed (or partially suppressed) by the addition of excess acyl substrate. In contrast, the rate of C28S inactivation by DTNB was accelerated to a much lesser extent by succinyl- or acetoacetyl-CoA, and C28S was inactivated less rapidly than wild-type SCOT or C196S under all conditions tested.

To assess the reversibility of SCOT inactivation, we examined whether the enzyme could be reactivated by adding DTT at various times during the incubation with DTNB.

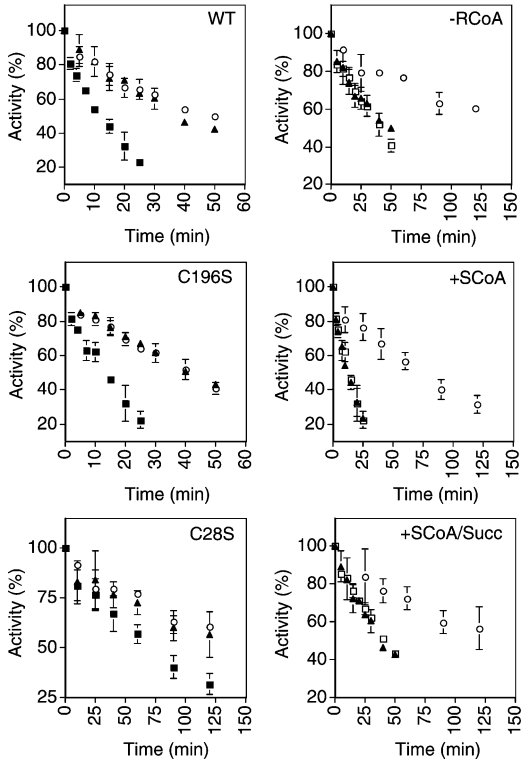

FIGURE 1: Kinetics of inactivation by DTNB in the presence of succinyl-CoA and succinate. Left panels: Graphs comparing enzyme activities in the absence of substrates (open circles) and in solutions containing succinyl-CoA (solid squares) or succinyl-CoA plus succinate (solid triangles), determined for wild-type SCOT (WT) (top panel), C196S (middle panel), and C28S (bottom panel). Right panels: Graphs comparing enzyme activities of WT (closed triangles), C196S (open squares), and C28S (open circles), determined in the absence of substrates (top panel) and in solutions containing succinyl-CoA (+SCoA, middle panel) or succinyl-CoA plus succinate (+SCoA/Succ, bottom panel). The graphs in the left and right panels are different representations of the same data sets. Enzyme activity is expressed as a percentage of the initial activity, and error bars correspond to the standard deviation ($N = 2-5$).

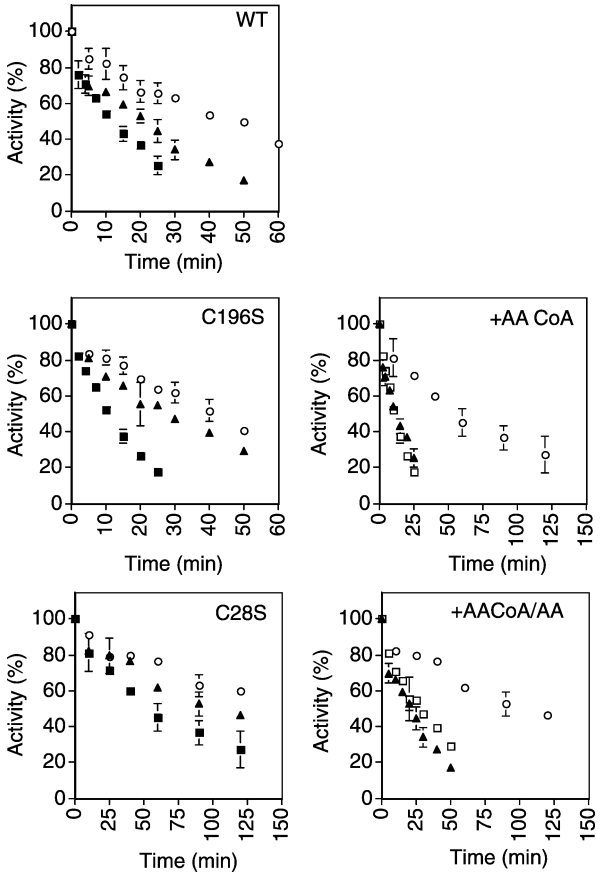

FIGURE 2: Kinetics of inactivation by DTNB in the presence of acetoacetyl-CoA and acetoacetate. Left panels: Graphs comparing enzyme activities in the absence of substrates (open circles) and in solutions containing acetoacetyl-CoA (solid squares) or acetoacetyl-CoA plus acetoacetate (solid triangles), determined for WT (top panel), C196S (middle panel), and C28S (bottom panel). Right panels: Graphs comparing enzyme activities of WT (closed triangles), C196S (open squares), and C28S (open circles), determined in solutions containing acetoacetyl-CoA (+AACoA, middle panel) or acetoacetyl-CoA plus acetoacetate (+AACoA/AA, bottom panel). The graphs in the left and right panels are different representations of the same data sets. Enzyme activity is expressed as a percentage of the initial activity, and error bars correspond to the standard deviation ($N = 2-4$).

Recovery of enzyme activity in the presence of DTT would suggest that inactivation by DTNB was due to steric hindrance resulting from the covalent attachment of TNB to a cysteine residue. Failure to reverse enzyme inactivation with DTT would suggest that inactivation by DTNB was due to protein unfolding following the attachment of TNB (i.e., inactivation via an unfolding mechanism should be irreversible, even in the presence of DTT). The addition of DTT had little effect on the activity of wild-type SCOT or C196S treated with DTNB in the absence of acyl-CoA substrate (Figure 3). Samples of wild-type SCOT or C196S that had been partially inactivated by DTNB in the presence of succinyl- or acetoacetyl-CoA were substantially reactivated upon treatment with DTT. For instance, although only ~20−30% of the initial activity of these two variants remained after incubation for 25 min with acyl-CoA and DTNB, ~60−70% of the initial activity was restored after the addition of DTT. In contrast, the inactivation of C28S by DTNB in the presence or absence of acyl-CoA was not reversed under reducing conditions.

In addition to assaying SCOT activity, we monitored the reaction of DTNB with cysteine residues by measuring the increase in A_{412} over time. Wild-type SCOT reacted with DTNB more rapidly in the presence of succinyl- or acetoacetyl-CoA than in the absence of acyl-CoA (Table 2; Supporting Information Figures S1 and S2). The accelerating effect of acyl-CoA was abolished by the addition of excess acyl substrate. Similar results were obtained with C196S, although the magnitude of the increase in A_{412} was only evident during the first ~15 min of the incubation and was less pronounced than for the wild-type enzyme (Table 2; Supporting Information Figures S1 and S2). In contrast to wild-type SCOT and C196S, C28S did not react more rapidly with DTNB in solutions containing acyl-CoA. The rate of the reaction was lower for C28S than wild-type SCOT or C196S under all conditions tested, and very little increase in A_{412} was observed when C28S was incubated with DTNB in the presence of acyl-CoA and excess acyl substrate (Table 2; Supporting Information Figures S1 and S2).

In summary, the rate of the reaction between C28S and DTNB (determined by monitoring enzyme activity and the increase in A_{412}) was not enhanced upon the formation of E−CoA. The inactivation of C28S by DTNB was irreversible under all conditions, similar to the inactivation of wild-type

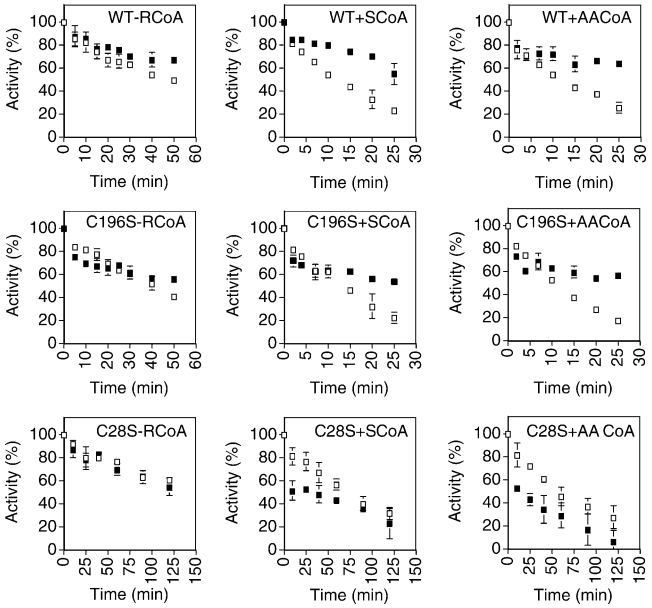

FIGURE 3: Effects of DTT on the inactivation of wild-type and mutant SCOT by DTNB. Graphs showing enzyme activities in the absence of reductant (open squares) or after DTT treatment (solid squares). Enzyme activities were determined for WT (top row), C196S (middle row), and C28S (bottom row), in the absence of substrates (left column) and in solutions containing succinyl-CoA (middle column) or acetoacetyl-CoA (right column). Enzyme activity is expressed as a percentage of the initial activity, and error bars correspond to the standard deviation ($N = 2-4$).

Table 2: Extent of Modification of SCOT by DTNB during the First 25 Min of Incubation in the Absence or Presence of Substrates[a]

	SCOT	C28S mutant	C196S mutant
−substrate	0.95	0.28	0.77
+succinyl-CoA	1.6	0.29	0.71
+succinyl-CoA + succinate	0.85	0.067	0.55
+acetoacetyl-CoA	1.7	0.18	0.68
+acetoacetyl-CoA + acetoacetate	0.87	0.067	0.63

[a] The data are presented as the moles of DTNB consumed per mole of enzyme subunit.

SCOT and C196S treated with DTNB in the absence of acyl-CoA substrate. From all of these observations, it was concluded that Cys 28 is Cys X, the cysteine residue located near the active site of SCOT.

To further investigate the role of Cys 28 during catalysis, this residue was mutated to alanine. In contrast to serine, the alanine residue would not have the potential to form a hydrogen bond with its side chain. In addition, the smaller side chain would contrast with both the cysteine and serine residues. The specific activity of the C28A mutant protein was 6 μmol min^{-1} mg^{-1}, similar to that of the C28S mutant protein. Surprisingly, k_{cat} for the C28A mutant protein in the forward direction was more than 10-fold lower than that for either wild-type SCOT or the C28S mutant (Table 1). It was partially offset by lower values for K_M for both acetoacetyl-CoA and succinate. In the reverse direction, k_{cat} for the C28A mutant protein was only 3-fold lower than k_{cat} for wild-type SCOT, contrasting with the results for the C28S mutant protein, and the values of K_M were similar to those for the wild-type SCOT.

Table 3: Statistics for the Crystallographic Data and Models of the C28S and C28A Mutant Proteins

	mutant protein	
	C28S	C28A
wavelength (Å)	1.11	1.07
space group	$P2_1$	$P2_1$
cell dimensions		
a (Å)	57.0	58.4
b (Å)	264.4	262.5
c (Å)	61.4	60.8
α, γ (deg)	90	90
β (deg)	109.8	109.6
resolution range (Å)	20−2.0	100−2.05
no. of measurements	384782	298185
no. of unique reflections	114144	95166
R_{merge}[a]	0.137	0.113
high-resolution shell	0.242	0.257
$\langle I_{avg}\rangle/\langle\sigma(I_{avg})\rangle$[b]	10.4	11.3
high-resolution shell	2.4 (2.03−2.00)	1.9 (2.09−2.05)
completeness (%)	95.1	92.5
high-resolution shell	68.2 (2.03−2.00)	60.8 (2.09−2.05)
Wilson *B*-factor	20.9	19.6
R_{work}[c] (%)	22.1	23.0
high-resolution shell	31.5 (2.09−2.00)	34.5 (2.15−2.06)
R_{free}[d] (%)	27.5	27.2
high-resolution shell	35.3 (2.09−2.00)	33.6 (2.15−2.06)
no. of protein atoms	14286	14298
total no. of atoms	15110	14588
no. of water molecules	823	290
heteroatoms	1 (Cl^-)	0
average *B*-factor	26.8	40.1
rmsd from ideal geometry		
bond lengths (Å)	0.013	0.006
bond angles (deg)	1.8	1.4
Ramachandran plot		
no. in most favorable regions (%)	1470 (92.0)	1461 (91.4)
no. in additionally allowed regions (%)	117 (7.3)	128 (8)
no. in generously allowed regions (%)	6 (0.4)	5 (0.3)
no. in disallowed regions (%)	4 (0.3)	4 (0.3)

[a] $R_{merge} = (\Sigma\Sigma|I_i - \langle I\rangle|)/\Sigma\Sigma\langle I\rangle$, where I_i is the intensity of an individual measurement of a reflection and $\langle I\rangle$ is the mean value for all equivalent measurements of this reflection. [b] $\langle I\rangle$ is the mean intensity for all reflections; $\langle\sigma(I)\rangle$ is the mean sigma for these reflections. [c] *R*-factor $= \Sigma||F_o| - |F_c||/\Sigma|F_o|$. [d] *R*-factor based on data excluded from the refinement (~5%).

To investigate the structural differences between wild-type SCOT and the Cys 28 mutants, the C28S and C28A mutant proteins were crystallized, and their structures were determined using X-ray crystallography. The structure of the C196S mutant protein was not pursued, since the catalytic activity of this mutant was similar to that of wild-type SCOT and we had shown that Cys 196 was not Cys X. The statistics for the two data sets and the models are presented in Table 3. Electron density at the site of the mutation for the C28S mutant protein is shown in Figure 4A. The structure of the C28S mutant shows that Oγ of the serine residue adopts a different position than Sγ of the cysteine residue in wild-type SCOT (Figure 4B). X_1 for Ser 28 in the four monomers in the asymmetric unit of the crystals ranged from 54° to 80°, in contrast to the values between −171° and −174° for Cys 28 (*13*, *39*). In the conformation adopted by the serine residue, the side chain hydroxyl donates a hydrogen bond to the carbonyl oxygen atom of Phe 25 (Figure 4). It accepts a hydrogen bond from a water molecule, which is also within

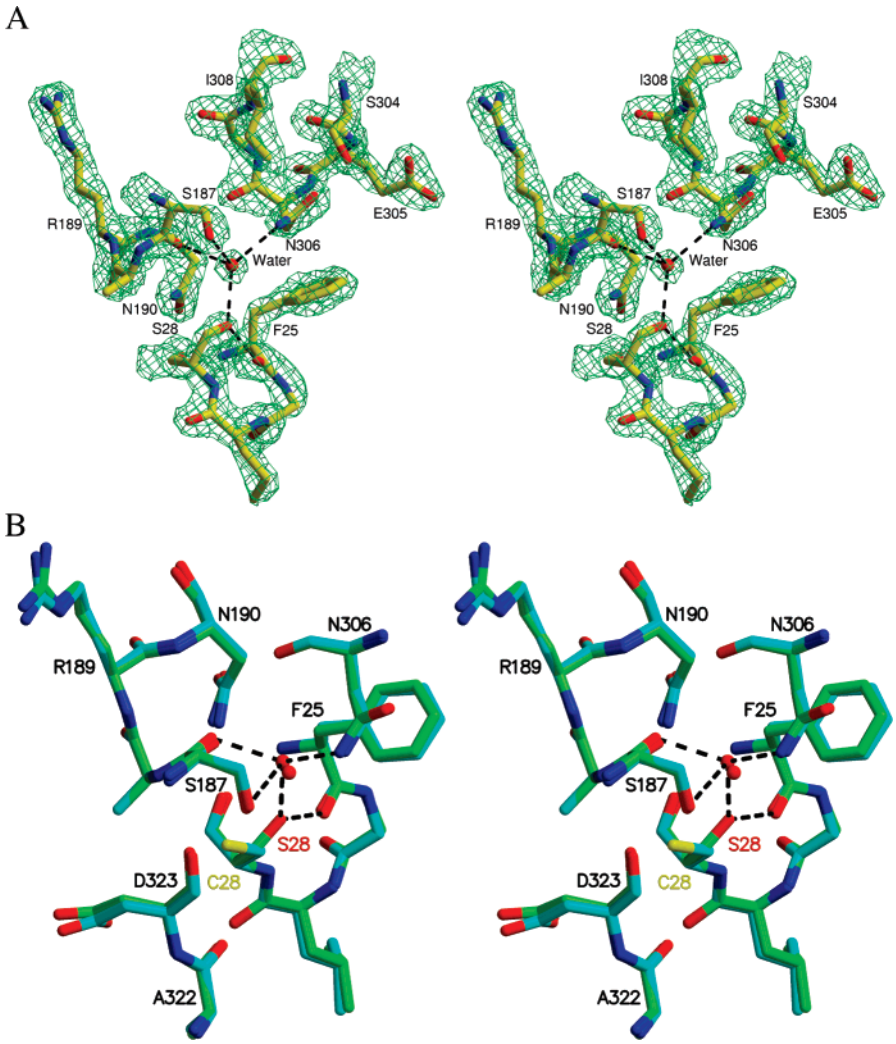

FIGURE 4: C28S mutant protein in the vicinity of the mutation. (A) Stereoview of the electron density for the C28S mutant protein. The model is drawn as sticks colored according to atom type: yellow for carbon, red for oxygen, and blue for nitrogen. The SIGMAA-weighted (*45*) $2F_o - F_c$, α_c electron density map is contoured at 1.5σ and shaded green. Black dashed lines show hydrogen-bonding interactions for Ser 28 and the water molecule. This figure was drawn using the programs XFIT (*31*) and RASTER3D (*46*). (B) Stereoview of the superposition of wild-type SCOT and the C28S mutant protein. The models are drawn as sticks colored according to atom type: yellow for sulfur, red for oxygen, blue for nitrogen, green for carbon in the C28S mutant, and cyan for carbon in the wild type. Black dashed lines show hydrogen-bonding interactions. This figure as well as Figures 5−7 was drawn using the programs MOLSCRIPT (*47*) and RASTER3D (*46*).

hydrogen-bonding distance of the two oxygen atoms of Ser 187 and the side chain nitrogen of Asn 306 (Figure 4). In the high-resolution structure of wild-type SCOT (*39*), there is an equivalent water molecule 3.3 Å from the sulfur and within hydrogen-bonding distances of the same residues, but the C28A mutant protein does not have a water molecule in the similar position.

The crystal structure of the C28S mutant protein shows a chloride ion bound in one of the four copies in the asymmetric unit. The electron density was interpreted as a chloride ion based on the peak height and its position. The chloride ion interacts with the side chains of Lys 329, Asn 51, and Asn 52 (Figure 5) and with a water molecule. Lys 329 adopts a different side chain conformation to form this interaction, since in the other molecules Nζ is hydrogen-bonded to the side chains of Glu 79 and Glu 241. The backbone atoms of residues 77−79 are also in different conformations, occupying the space vacated by Lys 329 when the lysine side chain interacts with the chloride ion. The structural changes are propagated from these residues to the α-helix that follows them in the polypeptide chain.

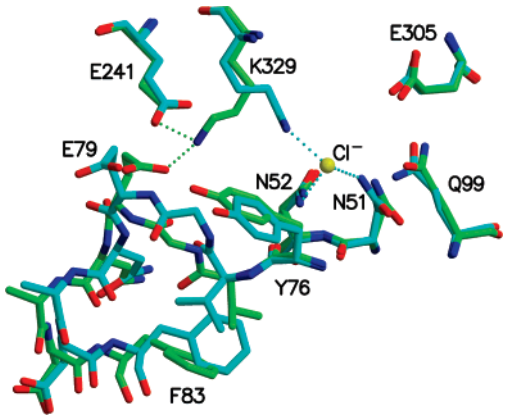

FIGURE 5: Comparison of the conformations of Lys 329 and nearby residues in two of the monomers, chain A and chain B of the C28S mutant protein. In chain A, Lys 329 interacts with a chloride ion, labeled Cl^-, while in chain B it interacts with two glutamate residues. The model is drawn as sticks colored according to atom type: red for oxygen, blue for nitrogen, yellow for chloride, cyan for carbon in chain A, and green for carbon in chain B.

DISCUSSION

The experiments contrasting the labeling of the C28S and C196S mutant proteins and wild-type SCOT clearly show that Cys 28 is the cysteine residue exposed on binding CoA in E−CoA. In each experiment, labeling of the C196S mutant protein was similar to that of wild-type SCOT, while differences appeared for the C28S mutant protein. However, while the data from measurements of A_{412} do support our conclusion that Cys 28 is Cys X, they also indicate that formation of E−CoA affects the exposure of Cys 196. In the presence of acyl-CoA, ~1.7 cysteine residues per subunit of wild-type SCOT reacted with DTNB after a 25 min incubation (Table 2; Supporting Information Figures S1 and S2), i.e., by the end of the rapid inactivation phase (Figures 1 and 2). Because only 0.3 cysteine residue per subunit of the C28S mutant protein reacted with DTNB under identical conditions (Table 2; Supporting Information Figures S1 and S2), we conclude that the presence of Cys 28 accounts for most of the reactivity of wild-type SCOT with DTNB in solutions containing acyl-CoA. However, Cys 28 is not *sufficient* for this reactivity, given that only 0.7 cysteine residue per mole of C196S reacted with DTNB during a 25 min incubation in the presence of acyl-CoA, compared to 1.7 cysteine residues per subunit of wild-type SCOT under identical conditions (Table 2; Supporting Information Figures S1 and S2). These findings are consistent with a model in which (i) Cys 28 of wild-type SCOT becomes exposed upon the formation of E−CoA and (ii) the rapid reaction of Cys 28 with DTNB causes additional conformational changes leading to the exposure and enhanced reactivity of Cys 196. Although Cys 196 reacts with DTNB under these conditions, our observation that wild-type SCOT and C196S lose activity at similar rates in the presence of acyl-CoA (Figures 1 and 2) indicates that the modification of Cys 196 contributes little to the rapid inactivation of E−CoA. So although Cys 196 is being modified, it does not affect catalysis.

The A_{412} data also provide insight into the degree of exposure of Cys 28 and Cys 196 in the Michaelis complex. The Michaelis complex is mimicked by using saturating amounts of the acyl-CoA and carboxylate substrates. Under these conditions, the enzyme exists primarily as two rapidly exchanging Michaelis complexes:

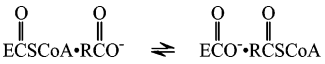

Two results suggest that wild-type SCOT adopts a different conformation in the Michaelis complex than in the E−CoA intermediate. First, the C28S mutant protein failed to react appreciably with DTNB in the presence of acyl-CoA and excess acyl substrate. The stoichiometry of this reaction was uncertain because the absorbance values were only slightly above background and varied with drift in the instrument (Supporting Information Figures S1 and S2). In contrast, the C28S mutant protein reacted with DTNB in solutions containing succinyl- or acetoacetyl-CoA without excess succinate or acetoacetate. Second, the absorbance produced by the C196S mutant protein and DTNB reached higher levels in the presence of acyl-CoA and excess carboxylate substrate than in the presence of acyl-CoA alone, suggesting that Cys 196 contributed less to the reaction with DTNB in the Michaelis complex than in E−CoA. These observations are consistent with a model in which Cys 28 is the primary exposed cysteine residue in the Michaelis complex, although it is less exposed under these conditions than in E−CoA. The reaction between Cys 28 and DTNB triggers conformational changes leading to the exposure and enhanced reactivity of other cysteine residues. The modification of Cys 28 induces less exposure of Cys 196 relative to cysteine residues at positions 417, 426, and 465 in the Michaelis complex than in E−CoA.

The identification of Cys 28 as Cys X is consistent with the observations that the C28S and C28A mutant proteins were less active than wild-type SCOT. On the basis of the labeling with the cyano group of NTCB, it was known that the essential cysteine residue of SCOT does not fulfill a direct mechanistic role, since covalent attachment of a cyano group to Cys 28 did not alter the enzyme's catalytic function (*10*). This leaves the question of what this residue's role is and why changing it to Ser or Ala would reduce activity. The structure of the C28S mutant protein shows that replacing Sγ with a hydroxyl group does change the hydrogen bonding in this region. The turn that includes Cys 28 and Phe 25 would be made more rigid by the change to Ser, since Ser donates a hydrogen bond to the carbonyl oxygen of Phe 25 (Figure 4). A second hydrogen bond formed between Ser 28 and the water molecule would also anchor this loop. The fact that adding a cyano group to Cys 28 does not reduce the activity of the enzyme indicates that a slightly larger side chain than that of cysteine can be accommodated (*10*). The crystal structure suggests that the cyano group could replace the water molecule. The C28A mutant protein is a suitable contrast to Ser, since Ala has no potential to form the hydrogen bonds. However, Ala is smaller than both Ser and Cys. The smaller side chain of the C28A mutant protein leads to only very small differences in the crystal structure. From the crystal structure, it is not evident why the C28A mutant is less active than wild-type SCOT, but it must be because of the absence of the thiol group, either due simply to the smaller size of Ala or due to the loss of the electrostatic properties of the thiol.

The interaction between Lys 329 and the chloride ion seen in the crystal structure for one monomer of the C28S mutant protein supports the view that Lys 329 interacts with at least one of the substrates. Three pieces of indirect evidence had led to the suggestion that a protonated amine forms part of the binding site for the carboxylate of one of the substrates (*40*). First, the enzyme is inhibited by monovalent anions (*8*). Second, the enzyme is irreversibly inactivated by acylation, but this reaction does not occur at neutral pH where a lysine side chain would be protonated and unreactive (*8*). Third, at low concentrations of succinate where the reaction of E−CoA with succinate would be rate determining, the plot of activity versus pH is bell-shaped with a pK of 8.4 for the upper limb, consistent with the pK_a for a lysine side chain (*41*). On the basis of the initial crystal structure of SCOT, it was suggested that this lysine residue was Lys 329 (*13*). Like the substrates acetoacetate and succinate, the chloride ion is negatively charged, so it would be attracted to the substrate-binding site. Sodium chloride is one of the salts known to inhibit SCOT: a 10 mM solution of sodium chloride was shown to inhibit SCOT by 24% (*8*). The inhibitory effect of the sodium salts were in the order $SCN^- > ClO_4^- > I^- \sim Br^- > Cl^- > F^-$ while the type of cation

had no effect, indicating that the anion was the inhibitor. In the crystallization solution, the chloride concentration would be greater than 100 mM because Tris-HCl was used as the buffer and because the protein sample contained KCl. At this concentration, chloride would be expected to partially inhibit SCOT, and this correlates well with seeing the chloride ion bound to only one of the four monomers. Our view is that this monomer shows the structure in an inhibited form. On the basis of the binding site for the chloride ion, we would predict that Asn 51 and Asn 52, in addition to Lys 329, interact with the substrate (Figure 5). Gln 99 had been postulated to serve a role in stabilizing the oxyanions of the tetrahedral intermediates based on the structure of glutaconate CoA-transferase (*42*), and that view is supported by its proximity to the chloride ion-binding site. The 6 Å distance between Lys 329 and Gln 99 would require Lys 329 to interact with the distal carboxylate of succinate/succinyl-CoA or the carbonyl of acetoacetate/acetoacetyl-CoA, not the carboxylate that forms the thioester with CoA and Glu 305.

In the crystal structure of SCOT, Cys 28 is buried, and there would have to be a conformational change for it to be labeled by NTCB or DTNB. In addition to the residues shown in Figure 4, Cys 28 is in contact with Ala 322, Asp 323, and Ile 325, as shown in Figure 6. This figure also shows Lys 329 since this residue is near the end of the loop covering Cys 28. In contrast, for the protein YdiF, the residue equivalent to Cys 28, Ile 40, is exposed to the solvent both in the structure of YdiF alone and in the covalent complex with CoA. This is because there is a much shorter loop here in YdiF, from residue 341 to residue 347 (*14*), where SCOT has 16 residues from 314 to 329. This loop is likely important in providing the substrate specificity of SCOT. In the structure of YdiF alone, as well as in the structure of its covalent complex with CoA, most of the residues of this loop were not modeled because there was no electron density for them. In SCOT, the movement of residues 325−329 would provide access to Cys 28 (Figure 6), and this must be what occurs on forming the covalent complex with CoA to allow for the chemical modification of Cys 28 by DTNB or NTCB. In the crystal structure of SCOT, Ile 325 forms hydrogen bonds with Ser 187 and Asn 306, both of which hydrogen bond to the water molecule shown in Figure 4. The hydrogen bonds to Ile 325 would have to be broken to release the residues shielding Cys 28.

Although we had believed that the mutation of Cys 28 to Ser would not affect catalysis, we discovered that it does change the interactions with Ile 325, and we now know that this would lead to a different stability for the loop that covers Cys 28 and includes Lys 329. The kinetic analyses (Table 1) show weaker binding for only one of the substrates, succinate, and only with the C28S mutant. Our interpretation of the catalytic mechanism is that acetoacetyl-CoA reacts with the enzyme to form the E−CoA intermediate, with the enzyme changing conformation through movement of the loop, minimally residues 325−329, to expose Cys 28. In this conformation, the enzyme could be rapidly inactivated by DTNB. We speculate that when succinate is present to react with E−CoA, the loop is reorganized to interact with succinate. This reorganization would block access to Cys 28, which is why high amounts of the acyl substrate block the labeling of Cys 28 even under conditions where the E−CoA intermediate is present.

The conclusion that the conformational change on binding acyl-CoA is in the region where the succinyl or acetoacetyl portion of the acyl-CoA binds leads to the question of whether this is the only conformational change on forming the covalent complex between CoA and the active site glutamate residue. Although the structure of SCOT has yet to be determined with CoA covalently bound to Glu 305, the structure of this enzyme intermediate has been determined with YdiF. By analogy to that structure, CoA should extend out of the funnel and would be predicted to interact with residues in the carboxy-terminal portion of SCOT, as presented in Table 4. The structure of SCOT does not superpose well with the structure of YdiF when taken in their entireties [root mean squared deviation (rmsd) 2.1 Å based on 308 Cα atoms that superpose within 3.8 Å], but the superposition is much better if the amino- and carboxy-terminal domains are considered separately. The carboxy-terminal domains are expected to superpose better than the amino-terminal domains because the acyl portion of sub-

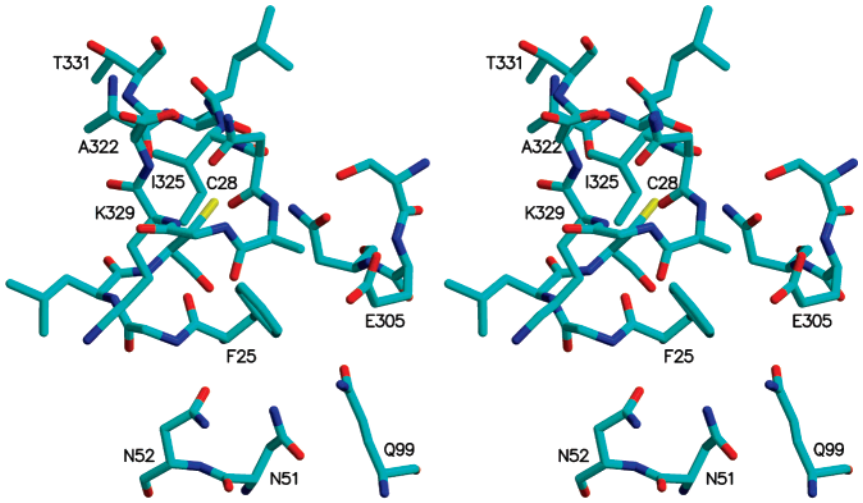

FIGURE 6: Stereoview of Cys 28 buried by the loop from Ala 322 to Thr 331. The model is drawn as sticks colored according to atom type: red for oxygen, blue from nitrogen, yellow for sulfur, and cyan for carbon. Residues that are proposed to be involved in binding and catalysis (for example, Lys 329, Asn 51, and Asn 52) are also included to show the locations of Cys 28 and the loop with respect to the active site.

Table 4: Residues of YdiF Interacting with CoA (*14*) and Their Proposed Analogues in SCOT

YdiF residues	interations	SCOT residues
Arg 288	diphosphates	Arg 263
Val 309-Gly 310-Ile 311	diphosphates	Ile 284-Gly 285-Ile 286
Glu 333	thioester	Glu 305
Ser 377	diphosphates	Gly 361
Ala 379-Glu 380	adenosine	Met 363-Gln 364
Phe 392	adenosine	Ile 376
Met 397	pantetheine	Lys 382
Thr 399	pantetheine	Met 384
Phe 402	pantetheine	Ala 387
Ile 405	thioester	Leu 390

strates is predicted to bind to the amino-terminal domain of each enzyme, and SCOT and YdiF do not bind the same substrates. Figure 7 shows part of the superposition of the amino-terminal domain of SCOT on the amino-terminal domain of YdiF (rmsd 2.0 Å based on 206 Cα atoms that superpose within 3.8 Å) and the carboxy-terminal domain of SCOT on the carboxy-terminal domain of YdiF (rmsd 1.6 Å based on 177 Cα atoms that superpose within 3.8 Å). The domain motion can be described as closure through a 17° rotation coupled with a 0.3 Å translation, as calculated using DynDom (*43*). If there were no conformational changes other than this motion, the amino- and carboxy-terminal domains of SCOT would clash in two regions, highlighted in Figure 7. In one of these, the clashes would be alleviated by the movement of residues 321−329, the same stretch of polypeptide that buries Cys 28 and must shift to allow chemical modification of this residue. The second region involves residues 374−386, the loop where the adenosine end of CoA is expected to bind. We propose that Ile 376 provides hydrophobic interactions with the adenine ring, analogous to Phe 392 of YdiF (Table 4). We speculate that this loop in SCOT would shift to interact with CoA and superpose better with the CoA-binding loop of YdiF. It would then not clash with the amino-terminal domain of SCOT. The conclusion is that this would be the second part of SCOT that changes conformation on binding CoA.

The identification of Cys 28 as the cysteine residue exposed on binding CoA leads us to propose a new model for catalysis by SCOT. On the basis of the first experiments

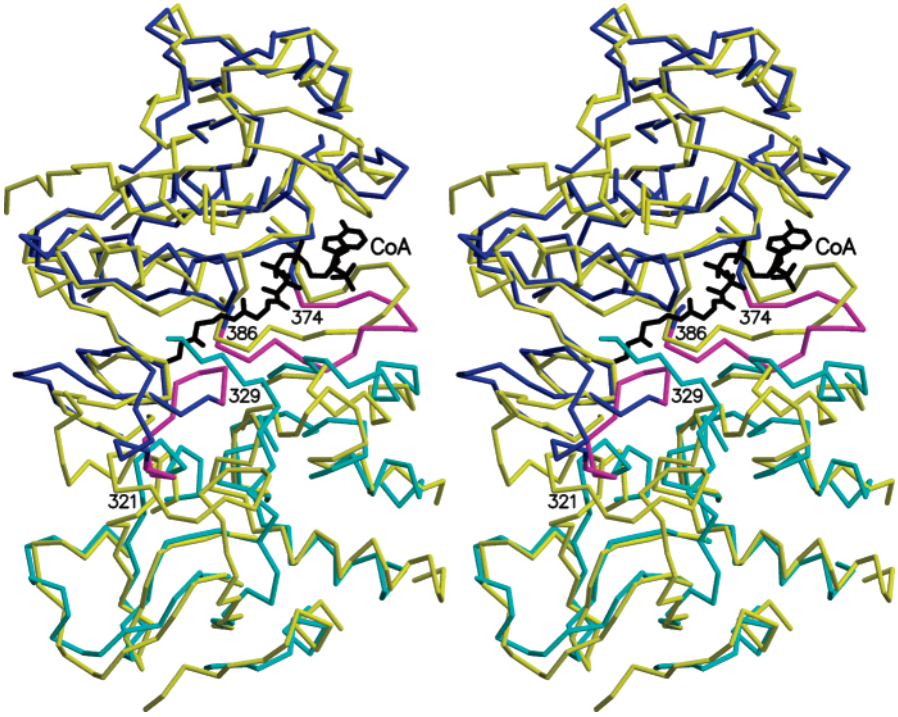

FIGURE 7: Stereoview of the superposition of the two domains of SCOT on YdiF. The Cα trace of YdiF is in yellow while the Cα trace of the amino-terminal domain of SCOT is in cyan and that of the carboxy-terminal domain is in blue, with the exception of residues 321−329 and 374−386. The Cα traces for these residues are in magenta to highlight the regions that must change conformation to prevent clashes when SCOT binds CoA. The bonds within the side chain of Glu 333 of YdiF and the covalently bound CoA are shown as black sticks. For clarity, only a slice of the superposition is shown.

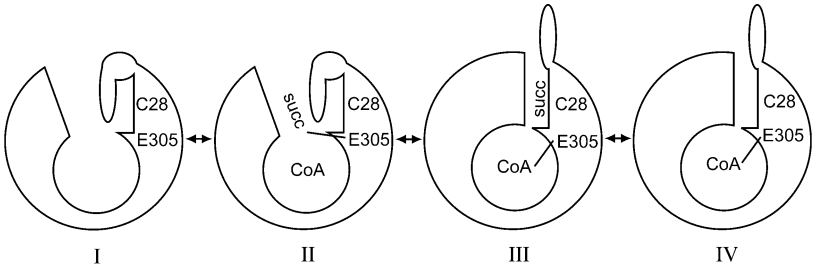

FIGURE 8: Model of catalysis by SCOT. I represents the open conformation. II represents the complex with succinate (Succ) linked to Glu 305 (E305), the anhydride intermediate. III and IV represent the closed conformation with CoA linked to Glu 305 as the thioester, with succinate shielding Cys 28 in III and Cys 28 exposed in IV.

inactivating SCOT with DTNB, White et al. drew an alligator model in which the enzyme is closed until it opens to form the thioester with CoA (*9*). In their model, the open state exposes the cysteine residue so that it can react with DTNB, unless the acyl group of either acyl-CoA or the carboxylate ion blocks it. The crystal structure of SCOT and our model of SCOT-CoA based on YdiF-CoA show that SCOT is first open, and it closes on binding CoA (Figure 8, I in contrast with III). We hypothesize that the succinyl group of succinyl-CoA interacts with Lys 329, Asn 51, and Asn 52 in the first step of catalysis, when the anhydride intermediate is formed with Glu 305 (represented in Figure 8 by II). In the second step, when CoA reacts with the anhydride intermediate to form the thioester, the loop protecting Cys 28 would lift, modifying the binding site for succinate (III). At the same time, SCOT would close since the loop no longer jams it open. Succinate would diffuse off the enzyme, exposing Cys 28 (IV), or be replaced by acetoacetate. Subsequently, acetoacetate would interact with the loop, pulling it into position to block Cys 28 and forcing the enzyme to open as the reaction continues in reverse through the second anhydride intermediate formed between acetoacetate and Glu 305. Formation of the anhydride intermediate releases CoA, which then reacts to form acetoacetyl-CoA as SCOT opens. We propose that the closure of the enzyme may serve to protect the thioester bond between Glu 305 and CoA, making it less likely to be hydrolyzed and making the transfer of CoA to the desired substrate more likely. Site-directed mutagenesis and structural information can now be used to test this new model, with the goal of understanding on the atomic level how SCOT uses the energy from binding CoA to undergo conformational changes that allow it to catalyze the transfer of CoA from succinyl-CoA to acetoacetate.

ACKNOWLEDGMENT

We thank Dr. Joseph Barycki for the gift of the plasmid expressing human L-3-hydroxyacyl-CoA dehydrogenase. We acknowledge Edward Brownie's excellent technical assistance in expressing and purifying both the human L-3-hydroxyacyl-CoA dehydrogenase and the C28S mutant protein for crystallization. We thank Dr. William T. Wolodko for critically reading and commenting on the manuscript.

SUPPORTING INFORMATION AVAILABLE

Two figures showing the kinetics of DTNB modication in the presence of succinyl-CoA and acetoacetyl-CoA. This material is available free of charge via the Internet at http://pubs.acs.org.

REFERENCES

1. Stern, J. R., Coon, M. J., and del Campillo, A. (1956) Enzymes of fatty acid metabolism. III. Breakdown and synthesis of β-keto fatty acids, *J. Biol. Chem. 221*, 1−14.
2. Stern, J. R., Coon, M. J., del Campillo, A., and Schneider, M. C. (1956) Enzymes of fatty acid metabolism IV. Preparation and properties of coenzyme A transferase, *J. Biol. Chem. 221*, 15−31.
3. White, H., and Jencks, W. P. (1976) Properties of succinyl-CoA: 3-ketoacid coenzyme A transferase, *J. Biol. Chem. 251*, 1708−1711.
4. Rochet, J. C., Brownie, E. R., Oikawa, K., Hicks, L. D., Fraser, M. E., James, M. N. G., Kay, C. M., Bridger, W. A., and Wolodko, W. T. (2000) Pig heart CoA transferase exists as two oligomeric forms separated by a large kinetic barrier, *Biochemistry 39*, 11291−11302.
5. Rochet, J. C., and Bridger, W. A. (1994) Identification of glutamate 344 as the catalytic residue in the active site of pig heart CoA transferase, *Protein Sci. 3*, 975−981.
6. Solomon, F., and Jencks, W. P. (1969) Identification of an enzyme-γ-glutamyl coenzyme A intermediate from coenzyme A transferase, *J. Biol. Chem. 244*, 1079−1081.
7. Falcone, A. B., and Boyer, P. D. (1959) Studies concerning the mechanism of action of acetoacetyl succinic thiophorase by use of O^{18}, *Arch. Biochem. Biophys. 83*, 337−344.
8. Hersh, L. B., and Jencks, W. P. (1967) Coenzyme A transferase. Kinetics and exchange reactions, *J. Biol. Chem. 242*, 3468−3480.
9. White, H., Solomon, F., and Jencks, W. P. (1976) Utilization of the inactivation rate of coenzyme A transferase by thiol reagents to determine properties of the enzyme-CoA intermediate, *J. Biol. Chem. 251*, 1700−1707.
10. Kindman, L. A., and Jencks, W. P. (1981) Modification and inactivation of CoA transferase by 2-nitro-5-(thiocyanato)benzoate, *Biochemistry 20*, 5183−5187.
11. Williams, W. A. (1990) Structure/function relationships within pig heart CoA transferase, Ph.D. Thesis, University of Minnesota.
12. Lin, T. W., and Bridger, W. A. (1992) Sequence of a cDNA clone encoding pig heart mitochondrial CoA transferase, *J. Biol. Chem. 267*, 975−978.
13. Bateman, K. S., Brownie, E. R., Wolodko, W. T., and Fraser, M. E. (2002) Structure of the mammalian CoA transferase from pig heart, *Biochemistry 41*, 14445−14462.
14. Rangarajan, E. S., Li, Y., Ajamian, E., Iannussi, P., Kernaghan, S. D., Fraser, M. E., Cygler, M., and Matte, A. (2005) Crystallographic trapping of the glutamyl-CoA thioester intermediate of family I CoA transferases, *J. Biol. Chem. 280*, 42919−42928.
15. Rochet, J.-C., Oikawa, K., Hicks, L. D., Kay, C. M., Bridger, W. A., and Wolodko, W. T. (1997) Productive interactions between the two domains of pig heart CoA transferase during folding and assembly, *Biochemistry 36*, 8807−8820.
16. Kunkel, T. A. (1985) Rapid and efficient site-specific mutagenesis without phenotypic selection, *Proc. Natl. Acad. Sci. U.S.A. 82*, 488−492.
17. Wang, W., and Malcolm, B. A. (1999) Two-stage PCR protocol allowing introduction of multiple mutations, deletions and insertions using QuikChange site-directed mutagenesis, *BioTechniques 26*, 680−682.
18. Sanger, F., Nicklen, S., and Coulson, A. R. (1977) DNA sequencing with chain-terminating inhibitors, *Proc. Natl. Acad. Sci. U.S.A. 74*, 5463−5467.
19. Sambrook, J., and Russell, D. W. (2001) *Molecular cloning: a laboratory manual*, 3rd ed., Cold Spring Harbor Laboratory Press, Cold Spring Harbor, NY.
20. Bridger, W. A., Ramaley, R. F., and Boyer, P. D. (1969) Succinyl coenzyme A synthetase from *Escherichia coli*, *Methods Enzymol. 13*, 70−75.
21. Howard, J. B., Zieske, L., Clarkson, J., and Rathe, L. (1986) Mechanism-based fragmentation of coenzyme A transferase. Comparison of alpha 2-macroglobulin and coenzyme A transferase thiol ester reactions, *J. Biol. Chem. 261*, 60−65.
22. White, H., and Jencks, W. P. (1976) Mechanism and specificity of succinyl-CoA:3-ketoacid coenzyme A transferase, *J. Biol. Chem. 251*, 1688−1699.
23. Whitty, A., Fierke, C. A., and Jencks, W. P. (1995) Role of binding energy with coenzyme A in catalysis by 3-oxoacid coenzyme A transferase, *Biochemistry 34*, 11678−11689.
24. Barycki, J. J., O'Brien, L. K., Strauss, A. W., and Banaszak, L. J. (2000) Sequestration of the active site by interdomain shifting, Crystallographic and spectroscopic evidence for distinct conformations of L-3-hydroxyacyl-CoA dehydrogenase, *J. Biol. Chem. 275*, 27186−27196.
25. Horecker, B. L., and Kornberg, A. (1948) The extinction coefficients of the reduced band of pyridine nucleotides, *J. Biol. Chem. 175*, 385−390.
26. Segel, I. H. (1975) *Enzyme kinetics: behavior and analysis of rapid equilibrium and steady state enzyme systems*, Wiley, New York.
27. Parratt, L. G. (1961) *Probability and experimental errors in science: an elementary survey*, Wiley, New York.
28. Ellman, G. L. (1958) A colorimetric method for determining low concentrations of mercaptans, *Arch. Biochem. Biophys. 74*, 443−450.

29. Otwinowski, Z., and Minor, W. (1997) Processing of X-ray diffraction data collected in oscillation mode, in *Methods in Enzymology* (Carter, C. W., Jr., and Sweet, R. M., Eds.) pp 307−326, Academic Press, New York.
30. Collaborative Computational Project, No. 4 (1994) The CCP4 suite: Programs for protein crystallography, *Acta Crystallogr. D50*, 760−763.
31. McRee, D. E. (1999) XtalView/Xfit−A versatile program for manipulating atomic coordinates and electron density, *J. Struct. Biol. 125*, 156−165.
32. Brunger, A. T. (1992) The free R value: a novel statistical quantity for assessing the accuracy of crystal structures, *Nature 355*, 472−474.
33. Brunger, A. T., Adams, P. D., Clore, G. M., Delano, W. L., Gros, P., Grosse-Kunstleve, R. W., Jiang, J.-S., Kuszewski, J., Jilges, N., Pannu, N. S., Read, R. J., Rice, L. M., Simonson, T., and Warren, G. L. (1998) Crystallography and NMR system (CNS): A new software system for macromolecular structure determination, *Acta Crystallogr. D54*, 905−921.
34. Hooft, R. W. W., Vriend, G., Sander, C., and Abola, E. E, (1996) Errors in protein structures, *Nature 381*, 272.
35. Laskowski, R. A., MacArthur, M. W., Moss, D. S., and Thornton, J. M. (1993) PROCHECK: A program to check the stereochemical quality of protein structures, *J. Appl. Crystallogr. 26*, 283−291.
36. Jones, T. A., Zou, J. Y., Cowan, S. W., and Kjeldgaard, M. (1991) Improved methods for building protein models in electron density maps and the location of errors in these models, *Acta Crystallogr. A47*, 110−119.
37. Guex, N., and Peitsch, M. C. (1997) SWISS-MODEL and the Swiss-PdbViewer: An environment for comparative protein modeling, *Electrophoresis 18*, 2714−2723.
38. Berman, H. M., Westbrook, J., Feng, Z., Gilliland, G., Bhat, T. N., Weissig, H., Shindyalov, I. N., and Bourne, P. E. (2000) The Protein Data Bank, *Nucleic Acids Res. 28*, 235−242.
39. Coros, A. M., Swenson, L., Wolodko, W. T., and Fraser, M. E. (2004) Structure of the CoA transferase from pig heart to 1.7 Å resolution, *Acta Crystallogr. D60*, 1717−1725.
40. Jencks, W. P. (1973) Coenzyme A transferases, in *The Enzymes* (Boyer, P. D., Ed.) pp 483−496, Academic Press, New York.
41. Solomon, F. (1970) Studies on the mechanism of action of succinyl-CoA:3-oxo-acid CoA-transferase, Ph.D. Thesis, Brandeis University.
42. Jacob, U., Mack, M., Clausen, T., Huber, R., Buckel, W., and Messerschmidt, A. (1997) Glutaconate CoA-transferase from *Acidaminococcus fermentans*: The crystal structure reveals homology with other CoA-transferases, *Structure 5*, 415−426.
43. Hayward, S., and Berendsen, H. J. C. (1998) Systematic analysis of domain motions in proteins from conformational change; New results on citrate synthase and T4 lysozyme, *Proteins: Struct., Funct., Genet. 30*, 144−154.
44. Moore, S. A., and Jencks, W. P. (1982) Formation of active site thiol esters of CoA transferase and the dependence of catalysis on specific binding interactions, *J. Biol. Chem. 257*, 10893−10907.
45. Read, R. J. (1986) Improved Fourier coefficients for maps using phases from partial structures with errors, *Acta Crystallogr. A42*, 140−149.
46. Merritt, E. A., and Bacon, D. J. (1997) Raster3D: Photorealistic molecular graphics, in *Methods in Enzymology* (Carter, C. W., Jr., and Sweet, R. M., Eds.) pp 505−524, Academic Press, New York.
47. Kraulis, P. J. (1991) MOLSCRIPT: A program to produce both detailed and schematic plots of protein structures, *J. Appl. Crystallogr. 24*, 946−950.

BI700828H